

0017-9310(94)00295-9

# Analytical solution of non-Darcian forced convection in an annular duct partially filled with a porous medium

S. CHIKH, A. BOUMEDIEN and K. BOUHADEF

Institut de Génie Mécanique, USTHB, BP 32, El Alia, Bab Ezzouar, Algeria

and

G. LAURIAT†

Laboratoire de Thermique, CNAM, 292 Rue St Martin, 75141 Paris Cedex 03, France

(Received 21 September 1994)

**Abstract**—An analytical solution is obtained for a fully developed, forced convection in a gap between two concentric cylinders. The inner is exposed to a constant heat flux and the outer is thermally insulated. A porous layer is attached to the inner cylinder. The effects of the permeability, thermal conductivity and the thickness of the porous material are investigated using a Brinkman–extended Darcy model. It is shown that there exists a critical thickness of the porous layer at which heat transfer is minimum in the case of low thermal conductivity materials, while this does not show for highly conducting materials. The obtained results show that increasing either the permeability or the thermal conductivity improves the heat transfer. Further, for highly permeable and conducting porous media, it may not be necessary to fill the gap completely to attain the maximum heat transfer.

## 1. INTRODUCTION

Heat transfer in porous media has received considerable attention and has been the field of a number of investigations during the last decade. The need for a better understanding of heat transport in these media is motivated by the numerous engineering applications encountered, in which a porous medium is present, such as geothermal systems, solid matrix heat exchangers, thermal insulation, oil extraction, storage of nuclear waste materials, etc.

A review of the related literature shows that most of the previous studies dealt with natural convection in cavities [1–6]. However, several authors [7–15] treated the annular geometry completely filled with a porous material and studied the natural convection heat transfer mode. Different numerical methods were used and the effects of parameters such as Rayleigh number and aspect ratio were discussed. Prasad *et al.* [16] performed an experimental work in steady state conditions and studied the effects of the same parameters.

Forced convection in porous filled ducts received less attention. Cheng and Hsu [17] treated the wall effects in a fully developed, forced convection in an annular duct with variable porosity, using a Brinkman model and a matched asymptotic expansion based method. A numerical work showing the channeling

effect was done by Vafai [18]. Poulikakos and Renken [19] considered two geometries, parallel plate channel and a cylinder, totally filled with a porous medium with prescribed temperatures at boundaries. Taking in account the porosity variation, inertial effects and the Brinkman term, they showed that the heat transfer rate was increased in comparison with Darcy model. A similar work applied to chemical reactors was done by Hunt and Tien [20]. Chou *et al.* [21] did an experimental–numerical comparison of the dispersion and channeling effects on heat transfer for a non-Darcian regime in a square channel completely filled with a porous medium. Wang and Du [22] studied and proposed a thermal dispersion model for forced convection in an annulus totally filled with a porous material.

Most of the reported work is either numerical or experimental. However, analytical solutions are presented for few specific cases. Vortmeyer and Schuster [23] used a variational method to solve the Brinkman equation. Vafai and Thiyagaraja [24] treated analytically the porous–fluid interface problems. Forced convection in a plane channel or a cylinder partially filled with a porous medium was the topic of the paper presented by Poulikakos and Kazmierczak [25]. An exact solution was proposed for the constant heat flux case, while a numerical solution was derived for a constant temperature case, for a thermally fully developed flow and a Brinkman model. Results were obtained for small values of effective thermal con-

---

† Author to whom correspondence should be addressed.

## NOMENCLATURE

$A$	constant in $N(r)$ expression	$T$	temperature
$B$	integration constant in $u_p(r)$	$u$	dimensionless axial velocity
$C$	integration constant in $u_p(r)$	$x$	axial position
$C_1$	integration constant in $u_f(r)$	$z$	transformed radial variable ( $z = r/\sqrt{Da}$ ).
$C_2$	integration constant in $u_f(r)$	Greek symbols	
$Da$	Darcy number ( $Da = K/H^2$ )	$\gamma$	constant in temperature expression
$D_h$	hydraulic diameter ( $D_h = 2H$ )	$\theta$	dimensionless temperature ( $\theta = (T_{wi}^* - T^*)/q_{wi}/h_i$ )
$e$	dimensionless porous layer thickness ( $e = e^*/H$ )	$\lambda$	binary parameter
$E$	constant in $N(r)$ expression	$\Lambda$	thermal conductivity ratio ( $\Lambda = k_e/k_f$ )
$F$	constant in $N(r)$ expression	$\mu$	dynamic viscosity
$H$	gap width ( $H = r_o^* - r_i^*$ )	$\phi$	function of $r^*$ in temperature expression.
$h_i$	heat transfer coefficient	Subscripts	
$k$	thermal conductivity	e	effective
$K$	permeability	f	fluid
$N(r)$	expression in $\theta$ ( $\theta = Nu_i N(r)$ )	i	inner
$Nu_i$	Nusselt number at the inner wall ( $Nu_i = h_i D_h/k_e$ )	o	outer
$Nu$	Nusselt number at the inner wall with respect to $k_f$ ( $Nu = h_i D_h/k_f$ )	p	porous.
$q_w$	wall heat flux	Superscript	
$r$	dimensionless radial position	*	dimensional quantities.
$s$	dimensionless radial position of the porous–fluid interface		

ductivity. Lauriat and Vafai [26] analyzed a forced convection in a parallel plate channel partially filled with a porous medium with a small effective thermal conductivity. An analytical solution was given for the Brinkman regime and approximate solutions were proposed when the Forchheimer term was taken in account. Vafai and Kim [27] worked out analytically a forced convection problem in a porous filled parallel plane channel using the Brinkman–Forchheimer–extended Darcy model.

In the present paper, an analytical solution for forced convection in an annular duct partially filled with a porous medium is derived. A porous layer is attached to the inner cylinder on which a constant heat flux is prescribed while the outer one is thermally insulated. The Brinkman–extended Darcy model is used for flow regime. Analytical solutions are presented for a hydrodynamically and thermally developed flow. It is shown that the porous material may be used for insulation or enhancement of heat transfer according to its physical properties, which are permeability and thermal conductivity. Thus, effects of parameters such as Darcy number, thermal conductivity ratio and porous layer thickness are considered.

## 2. HYDRODYNAMIC ANALYSIS

A fully developed flow, using the Brinkman–extended Darcy model is analyzed for the domain shown in Fig. 1. Under the following assumptions

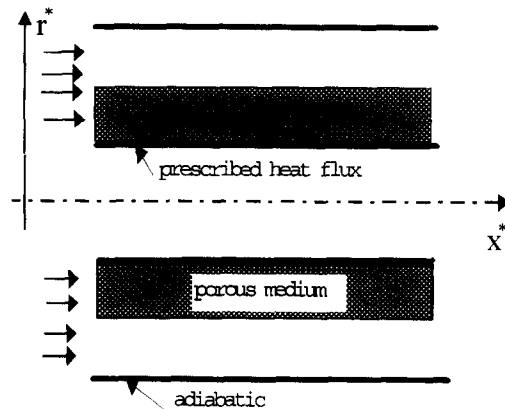


Fig. 1. Schematic of the physical domain.

$$\mu_e^* = \mu_f^* = \mu^*$$

$$\left(\frac{dp^*}{dx^*}\right)_p = \left(\frac{dp^*}{dx^*}\right)_f = \left(\frac{dp^*}{dx^*}\right)$$

Momentum equations for the porous and fluid regions are written as:

(i) in the porous medium:

$$0 = -\left(\frac{dp^*}{dx^*}\right) + \mu^* \frac{1}{r^*} \frac{d}{dr^*} \left( r^* \frac{du_p^*}{dr^*} \right) - \frac{\mu^*}{K} u_p^* \quad (1)$$

(ii) in the fluid layer:

$$0 = -\left(\frac{dp^*}{dx^*}\right) + \mu^* \frac{1}{r^*} \frac{d}{dr^*} \left( r^* \frac{du_f^*}{dr^*} \right) \quad (2)$$

with the following boundary conditions:

$$\text{at } r^* = r_i^* \quad u_p^* = 0$$

$$\text{at } r^* = r_o^* \quad u_f^* = 0$$

at the porous–fluid interface

$$r^* = r_i^* + e^* \quad u_p^* = u_f^*$$

$$\frac{du_p^*}{dr^*} = \frac{du_f^*}{dr^*} \quad (3)$$

Introducing the dimensionless variables defined as:

$$r = \frac{r^*}{H} \quad \text{where } H = r_o^* - r_i^* = \frac{D_h}{2}$$

and  $D_h$  is the hydraulic diameter

$$r_i = \frac{r_i^*}{H} \quad r_o = \frac{r_o^*}{H} \quad s = \frac{r_i^* + e^*}{H}$$

$$u = \frac{u^*}{\frac{H^2}{\mu^*} \left( \frac{dp^*}{dx^*} \right)} \quad Da = \frac{K}{H^2}$$

equations (1) and (2) become:

(i) in the porous medium:  $r_i \leq r \leq s$

$$\frac{1}{r} \frac{d}{dr} \left( r \frac{du_p}{dr} \right) - \frac{1}{Da} u_p = 1 \quad (4)$$

(ii) in the fluid region:  $s \leq r \leq r_o$

$$\frac{1}{r} \frac{d}{dr} \left( r \frac{du_f}{dr} \right) = 1. \quad (5)$$

The associated boundary conditions are:

$$\text{at } r = r_i \quad u_p = 0$$

$$\text{at } r = r_o \quad u_f = 0$$

$$\text{at } r = s \quad u_p = u_f$$

$$\frac{du_p}{dr} = \frac{du_f}{dr}. \quad (6)$$

### 2.1. Analytical solution

Equation (5) is easily integrated to yield the velocity distribution in the fluid, which is of the form

$$u_f(r) = \frac{r^2}{4} + C_1 \ln r + C_2. \quad (7)$$

Introducing a new variable  $z = r/\sqrt{Da}$ , equation (4) may be written as

$$\frac{d^2 u_p}{dz^2} + \frac{1}{z} \frac{du_p}{dz} - u_p = Da \quad (8)$$

which is a modified Bessel equation of zeroth order, with a non-zero right hand side. The solution of equation (8) is of the form

$$u_p(z) = BI_o(z) + CK_o(z) - Da \quad (9)$$

where  $I_o$  and  $K_o$  are the modified Bessel functions of zeroth order of first and second kind, respectively.

The constants  $C_1$ ,  $C_2$ ,  $B$  and  $C$  are determined using the boundary conditions and making use of the following properties of Bessel functions:

$$I'_o(z) = I_1(z)$$

and

$$K'_o(z) = -K_1(z). \quad (10)$$

$I_1$  and  $K_1$  are the modified Bessel functions of first order of first and second kind, respectively. After some algebraic calculation the constants are obtained as:

$$K_{oi}(s^2 - r_o^2) - \frac{s^2}{2} \ln\left(\frac{s}{r_o}\right) K_{oi} + Da(K_{oi} - K_{os})$$

$$B = \frac{-\frac{s}{\sqrt{Da}} \ln\left(\frac{s}{r_o}\right) K_{is} Da}{I_{os} K_{oi} - I_{oi} K_{os} - \frac{s}{\sqrt{Da}} \ln\left(\frac{s}{r_o}\right) (I_{is} K_{oi} + K_{is} I_{oi})} \quad (11)$$

$$C = \frac{Da}{K_{oi}} - \frac{I_{oi}}{K_{oi}} B \quad (12)$$

$$C_1 = \frac{s}{\sqrt{Da}} (BI_{is} - CK_{is}) - \frac{s^2}{2} \quad (13)$$

$$C_2 = -C_1 \ln(r_o) - \frac{r_o^2}{4}. \quad (14)$$

The modified Bessel functions  $K_{oi}$ ,  $I_{oi}$ ,  $K_{os}$ ,  $K_{is}$ ,  $I_{os}$  and  $I_{is}$  introduced in equations (11)–(14) stand for the values of the functions at the positions  $r_i/\sqrt{Da}$  and  $s/\sqrt{Da}$ , respectively.

### 3. THERMAL ANALYSIS

The analysis is carried out for a thermally fully developed flow. The governing energy equation is written as:

(i) in the porous medium:

$$\rho^* c_p^* u_p^* \frac{\partial T_p^*}{\partial x^*} = k_e \frac{1}{r^*} \frac{\partial}{\partial r^*} \left( r^* \frac{\partial T_p^*}{\partial r^*} \right) \quad (15)$$

(ii) in the fluid layer:

$$\rho^* c_p^* u_f^* \frac{\partial T_f^*}{\partial x^*} = k_f \frac{1}{r^*} \frac{\partial}{\partial r^*} \left( r^* \frac{\partial T_f^*}{\partial r^*} \right). \quad (16)$$

Introducing a binary parameter  $\lambda$ , which takes values of 1 in the porous medium and 0 in the fluid, the two previous equations may be combined into a single form as follows:

$$\rho^* c_p^* u^* \frac{\partial T^*}{\partial x^*} = \{ \lambda(k_e - k_f) + k_f \} \frac{1}{r^*} \frac{\partial}{\partial r^*} \left( r^* \frac{\partial T^*}{\partial r^*} \right). \quad (17)$$

The boundary conditions are:

$$\begin{aligned} \text{at } r^* = r_i^* \quad q_{wi} &= -k_c \frac{\partial T^*}{\partial r^*} \Big|_{r^*=r_i^*} \\ \text{at } r^* = r_o^* \quad q_{wo} &= 0 \\ \text{at } r^* = r_i^* + e^* \quad T_p^* &= T_f^* \\ &-k_c \frac{\partial T_p^*}{\partial r^*} = -k_f \frac{\partial T_f^*}{\partial r^*}. \end{aligned} \tag{18}$$

A dimensionless temperature  $\theta$ , a thermal conductivity ratio  $\Lambda$  and Nusselt number  $Nu_i$  are defined as:

$$\theta = \frac{T_{wi}^* - T^*}{q_{wi}/h_i} \quad \Lambda = \frac{k_c}{k_f} \quad Nu_i = \frac{D_h h_i}{k_c}.$$

Fully developed conditions implies that  $\partial T^*/\partial x^*$  is constant. Therefore equation (17) may be written as

$$\Lambda \cdot Nu_i \frac{r_i}{r_o + r_i} \frac{u}{\bar{u}} = \{ \lambda(1 - \Lambda) - 1 \} \frac{1}{r} \frac{\partial}{\partial r} \left( r \frac{\partial \theta}{\partial r} \right) \tag{19}$$

where  $T_{wi}^*$  and  $h_i$  are the wall temperature of the inner cylinder and the heat transfer coefficient, respectively.  $\bar{u}$  is the mean velocity over the whole cross section given by the relationship

$$\bar{u} = \frac{2}{r_o^2 - r_i^2} \left\{ \begin{aligned} &Bs\sqrt{Da} I_{1s} - Cs\sqrt{Da} K_{1s} - Da \frac{s^2}{2} \\ &- Br_i\sqrt{Da} I_{1i} + Cr_i\sqrt{Da} K_{1i} \\ &+ Da \frac{r_i^2}{2} + \frac{r_o^4}{16} + C_1 \frac{r_o^2}{4} + C_2 \frac{r_o^2}{2} \\ &-\frac{s^4}{16} - C_1 s^2 \frac{\ln s}{2} + C_1 \frac{s^2}{4} - C_2 \frac{s^2}{2} \end{aligned} \right\}. \tag{20}$$

The corresponding boundary conditions reduce to

$$\begin{aligned} \text{at } r = r_i \quad Nu_i &= 2 \frac{\partial \theta}{\partial r} \Big|_{r=r_i} \\ \text{at } r = r_o \quad \frac{\partial \theta}{\partial r} \Big|_{r=r_o} &= 0. \end{aligned} \tag{21}$$

At this point,  $Nu_i$  being unknown and function of the temperature profile, a non-linearity is introduced in equation (19) and, implicitly, in the boundary condition (21). A modification is then necessary and thus, since the regime is thermally fully developed, we can write

$$T^*(x^*, r^*) = \gamma x^* + \phi(r^*) \tag{22}$$

$\gamma$  being a constant, and

$$\theta = \frac{\gamma x^* + \phi(r_i^*) - \gamma x^* - \phi(r^*)}{q_{wi}/h_i} \tag{23}$$

or

$$\theta = \left( \frac{D_h h_i}{k_c} \right) \left\{ \frac{k_c}{q_{wi} D_h} (\phi(r_i^*) - \phi(r^*)) \right\} \tag{24}$$

$$\theta = Nu_i N(r). \tag{25}$$

$N(r)$  is a function of  $r$  given by the expression between brackets in equation (24). Making use of the dimensionless temperature, equation (21) is also modified and written as

$$\theta(r_i) = 0 \quad \text{or} \quad N(r_i) = 0. \tag{26}$$

Energy equation (19) is then transformed to

$$\left( \frac{\Lambda}{\lambda(1 - \Lambda) - 1} \frac{r_i}{r_i + r_o} \right) \frac{u}{\bar{u}} r = \frac{d}{dr} \left( r \frac{dN}{dr} \right) \tag{27}$$

with the boundary conditions

$$N(r_i) = 0 \quad \text{and} \quad \frac{dN}{dr} \Big|_{r=r_o} = 0 \tag{28}$$

or in another form of equation (27)

$$r^2 \frac{d^2 N}{dr^2} + r \frac{dN}{dr} = \left\{ \left( \frac{\Lambda}{\lambda(1 - \Lambda) - 1} \right) \left( \frac{r_i}{r_i + r_o} \right) \right\} \frac{u}{\bar{u}} r^2 \tag{29}$$

which is of the form of the Euler or Cauchy equation.

### 3.1. Analytical solution

Equation (29) is of the classical form

$$x^2 \frac{d^2 y}{dx^2} + ax \frac{dy}{dx} + by = S(x) \tag{30}$$

where  $a = 1$  and  $b = 0$ .

Let  $x = \exp(t)$ , then equation (30) becomes

$$\frac{d^2 y}{dt^2} + (a - 1) \frac{dy}{dt} + by = S(\exp(t)) \tag{31}$$

and its solution is given by

$$y = E + Ft + t \int S(e^t) dt - \int t S(e^t) dt. \tag{32}$$

The solution of equation (29) is then deduced and written as

$$N(r) = E + F \ln r + \ln r \int A \frac{u}{\bar{u}} r dr - \int A \frac{u}{\bar{u}} r \ln r dr \tag{33}$$

where  $A = -r_i/(r_i + r_o)$  and  $u$  given by equation (9) in the porous region and  $A = -r_i \Lambda/(r_i + r_o)$  and  $u$  given by equation (7) in the fluid.

The constants  $E$  and  $F$  for both regions are determined using the boundary conditions, equations (18), expressed in terms of  $N(r)$ .

After tough analytical integrations and employing recurrence formulas of the Bessel functions, we get

$$N_p(r) = E_p + F_p \ln(r) - \frac{r_i}{(r_i + r_o)\bar{u}} \times \left\{ B Da I_0\left(\frac{r}{\sqrt{Da}}\right) + C Da K_0\left(\frac{r}{\sqrt{Da}}\right) - \frac{Da}{4} r^2 \right\} \quad (34)$$

and

$$N_f(r) = E_f + F_f \ln(r) - \frac{r_i \Lambda}{(r_i + r_o)\bar{u}} \times \left\{ \frac{r^2}{64} + C_1 \frac{r^2}{4} \ln(r) - (C_1 - C_2) \frac{r^2}{4} \right\} \quad (35)$$

where the subscripts p and f indicate porous and fluid regions, respectively. The expressions of the constants  $E_p, F_p, E_f$  and  $F_f$  are given in the Appendix.

3.2. Determination of Nusselt number

Employing the relationship  $\theta = Nu_i N(r)$ , we may write

$$\int_{r_i}^{r_o} \theta u 2\pi r dr = Nu_i \int_{r_i}^{r_o} N(r) u 2\pi r dr \quad (36)$$

or

$$Nu_i = \frac{\int_{r_i}^{r_o} \theta u r dr}{\int_{r_i}^{r_o} N(r) u r dr} \quad (37)$$

Defining the bulk temperature and introducing the dimensionless temperature, we obtain

$$\int_{r_i}^{r_o} \theta u r dr = \bar{u} \left( \frac{r_o^2 - r_i^2}{2} \right) \quad (38)$$

and, hence,

$$Nu_i = \left( \frac{r_o^2 - r_i^2}{2} \right) \frac{\bar{u}}{\int_{r_i}^{r_o} N(r) u r dr} \quad (39)$$

Tough analytical calculations of different integrals (see Appendix) yield the Nusselt number.

4. RESULTS AND DISCUSSION

Results of flow field and heat transfer are presented in terms of velocity profiles and Nusselt numbers. The effects of parameters based on physical properties of the porous material such as Darcy number ( $Da$ ) and the thermal conductivity ratio ( $\Lambda = k_e/k_f$ ) are discussed. The effect of the porous layer thickness, varying from 0% to 100% of the gap, is also considered. All the results are presented for a radius ratio kept at a constant value ( $r_i/r_o = 0.5$ ). Qualitatively, the effects of the parameters considered are

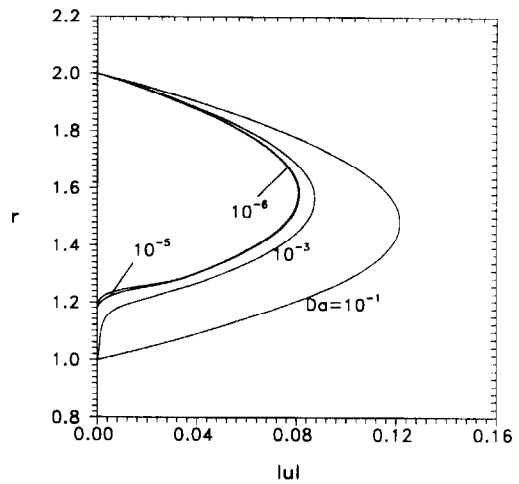


Fig. 2. Velocity profiles for different  $Da, e = 0.2$ .

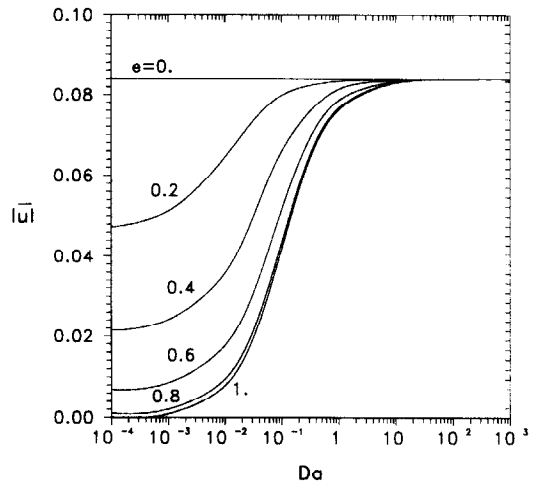
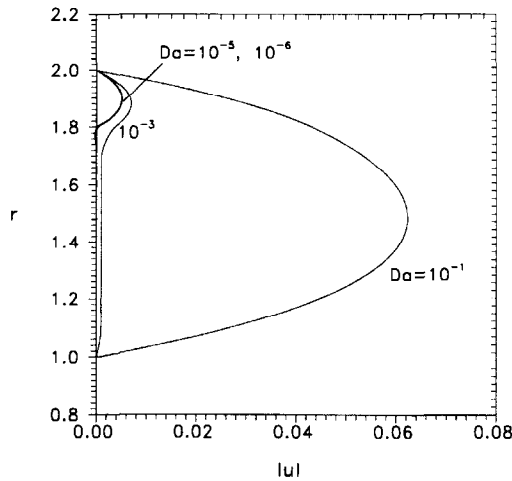
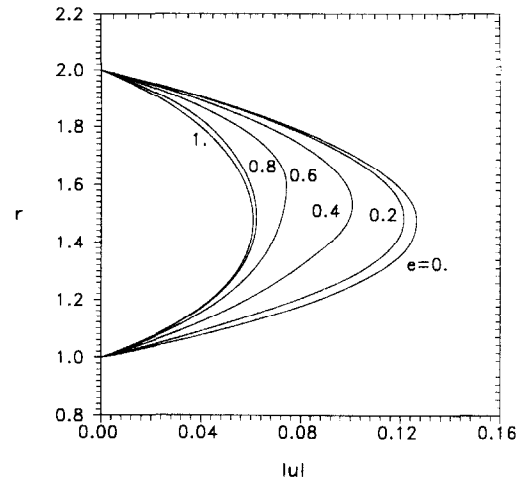
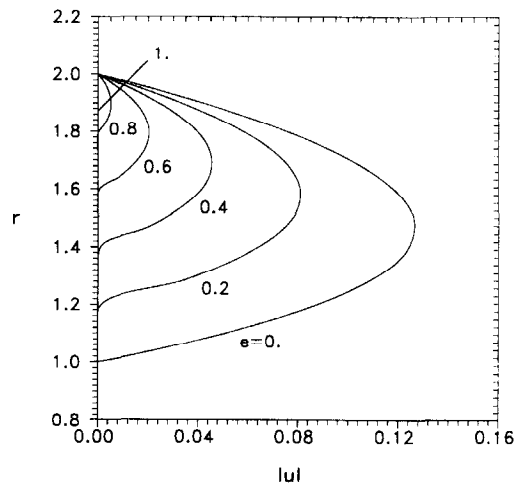
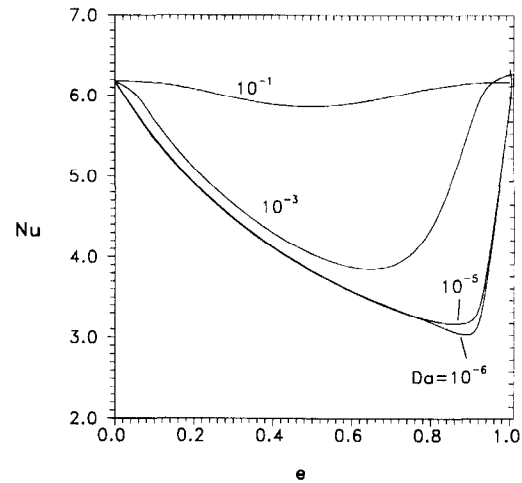


Fig. 3. Mean velocity as a function of  $Da$  for different thicknesses.

the same for any other value of the radius ratio. In order to compare heat transfer results to the case where no porous medium is present, the Nusselt number is redefined with respect to the thermal conductivity of the fluid. Figure 2 shows the velocity distribution for different values of  $Da$  when the porous layer occupies 20% of the channel. For small  $Da$ , i.e. low permeability, the porous material presents a high resistance to the flow; hence the velocity profile is flattened in that region, which basically corresponds to a Darcian regime for  $Da$  less than  $10^{-4}$ . As the permeability increases (higher  $Da$ ), this resistance to the flow decreases and the Brinkman-extended Darcy regime is obtained for  $10^{-4} < Da < 10$  as shown in Fig. 3 in which the average velocity is plotted against  $Da$ . The same effect is observed in Fig. 4, when 80% of the channel is filled with the porous medium. As in Fig. 2, it can be seen that, at higher  $Da$ , the resistance due to the porous matrix has no effect and a fluid velocity profile is recovered. The velocity profiles are

Fig. 4. Velocity profiles for different  $Da$ ,  $e = 0.8$ .Fig. 6. Velocity profiles for different porous layer thicknesses,  $Da = 10^{-1}$ .Fig. 5. Velocity profiles for different porous layer thicknesses,  $Da = 10^{-5}$ .Fig. 7. Nusselt number as a function of porous layer thickness for different  $Da$ ,  $k_c/k_f = 1$ .

presented in Figs. 5 and 6 for various porous layer thicknesses. It is shown that filling the annulus reduces the flow rate whether the permeability of the porous material is low or high.

Heat transfer results are presented in the remaining figures. Variations of Nusselt number as a function of the porous layer thickness, for different values of  $Da$ , are shown in Fig. 7 for a low thermal conductivity material ( $k_c/k_f = 1$ ) which may be used for insulation. For a given permeability, the Nusselt number decreases when the porous layer thickness increases, up to a critical value beyond which,  $Nu$  increases to end up at almost the same value as in the case of the completely porous channel. The physical explanation is that, when the porous layer thickness increases, the flow rate is reduced and hence the prescribed heat flux makes the wall temperature increase more than the mean temperature of the fluid. The Nusselt number, being inversely proportional to the temperature difference, decreases until the critical thickness is reached. Over this value, the inverse effect is produced,

that is the fluid mean temperature increases more than the wall temperature and thus  $Nu$  is augmented. Similar results were shown by Poulikakos and Kazmierczak [25] for a partially filled cylinder, by Lauriat and Vafai [26] for a parallel plate channel, by Campos *et al.* [5] and by others [1, 6]. It is worth noting that the limiting case of no porous medium ( $Nu = 6.18101$ ) agrees with results given in the literature [28]. The effect of permeability is also seen in this figure through the different values of  $Da$ . The more permeable is the medium, the higher is heat transfer and the lower is the critical thickness. One can deduce that there is no need to fill up the channel with the porous material to obtain the minimum heat transfer.

The critical thickness disappears as the porous material becomes more conducting, for any permeability, as shown in Fig. 8 ( $Da = 10^{-4}$  and  $10^{-2}$ ). Beyond a certain thermal conductivity value, which varies with the permeability, the presence of the porous medium enhances heat transfer. The Nusselt

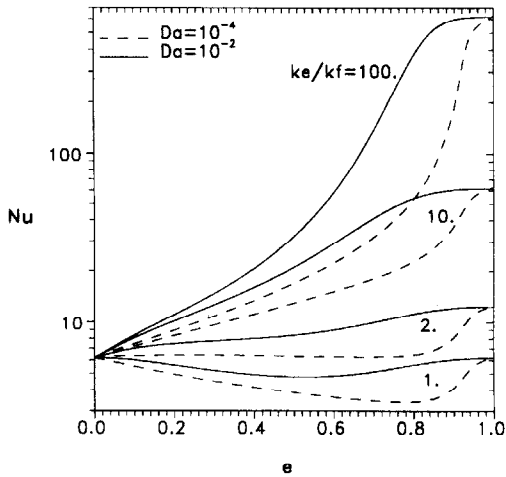


Fig. 8. Nusselt number as a function of porous layer thickness for different  $k_e/k_f$ ,  $Da = 10^{-4}$  and  $10^{-2}$ .

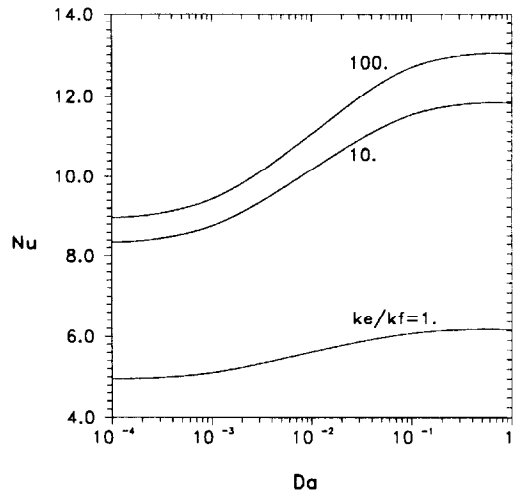


Fig. 10. Nusselt number vs Darcy number for different thermal conductivity ratios,  $e = 0.2$ .

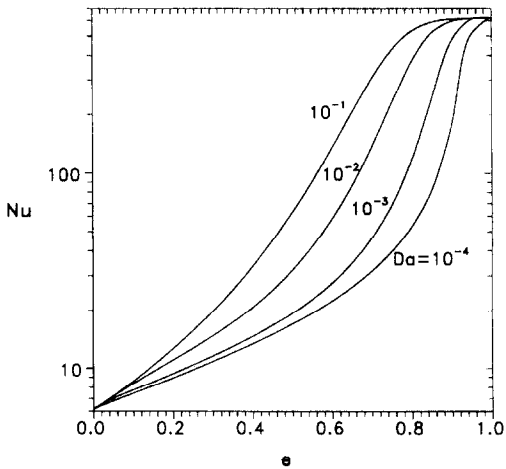


Fig. 9. Nusselt number vs porous layer thickness for different  $Da$ ,  $k_e/k_f = 100$ .

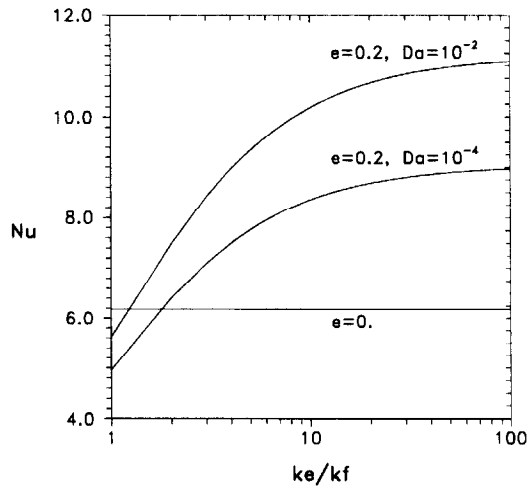


Fig. 11. Nusselt number vs thermal conductivity ratio,  $e = 0.2$ ,  $Da = 10^{-4}$  and  $10^{-2}$ .

number increases substantially, notably for a highly conducting material ( $k_e/k_f = 100$ ), up to nearly a constant value which is reached when approximately 85% of the annulus gap is filled (for  $Da = 10^{-1}$ ).

If the medium is more permeable, a higher  $Nu$  is obtained and the constant value is reached for smaller thicknesses. Thus, even with a highly conducting material, it is sufficient to fill the channel just to a critical thickness (about 85% for  $Da = 10^{-1}$ ) to reach the maximum heat transfer rate as shown in Fig. 9. Figure 10 shows both the effects of permeability and thermal conductivity of a porous layer which occupies 20% of the duct. It is clear that increasing either  $Da$  or thermal conductivity ratio improves the heat transfer.

In Fig. 11, the role played by the porous layer with respect to heat transfer is shown. For a relatively low permeability ( $Da = 10^{-4}$ ), the porous medium presents a resistance to heat transfer, unless the material is nearly twice as much conducting as the

fluid ( $k_e/k_f = 2$ ), beyond which point the medium enhances heat transfer. For a higher permeability material, it happens even at lower thermal conductivity ratio (about 1.6 for  $Da = 10^{-2}$ ).

### 5. CONCLUSION

Forced convection analysis is done in an annular duct partially filled with a porous medium. The presence of a porous layer is shown to present a resistance to the flow and heat transfer for low permeability materials. However, for highly conducting porous media, heat transfer is systematically augmented whatever the  $Da$  value is. It is also shown that, whether the porous material is used for insulation or for enhancement of heat transfer, there is no need to fill the gap completely, especially if the medium is highly permeable.

## REFERENCES

1. T. W. Tong and E. Subramanian, Natural convection in rectangular enclosure partially filled with a porous medium, *Proc. ASME/JSME Thermal Engineering Joint Conference*, Vol. 1, pp. 331–338 (1983).
2. C. Beckermann, S. Ramadhyani and R. Viskanta, Natural convection flow and heat transfer between a fluid layer and a porous layer inside a rectangular enclosure, *ASME J. Heat Transfer* **109**, 363–370 (1987).
3. C. Beckermann, R. Viskanta and S. Ramadhyani, Natural convection in vertical enclosures containing simultaneously fluid and porous layers, *J. Fluid Mech.* **186**, 257–284 (1988).
4. S. B. Sathe and T. W. Tong, Comparison of four insulation schemes for reduction of natural convective heat transfer in rectangular enclosures, *Int. Commun. Heat Mass Transfer* **16**, 795–802 (1989).
5. H. Campos, J. C. Morales, U. Lacoa and A. Campo, Thermal aspects of a vertical annular enclosure divided into a fluid region and a porous region, *Int. Commun. Heat Mass Transfer* **17**, 343–354 (1990).
6. V. Prasad, K. Brown and Q. Tian, Flow visualization and heat transfer experiments in fluid superposed porous layers heated from below, ASME, Winter Annual Meeting (1989).
7. C. E. Hickox and D. K. Gartling, A numerical study of natural convection in a vertical annular porous layer, ASME, paper 82-HT-68, pp. 1–7 (1982).
8. M. A. Havstad and P. J. Burns, Convective heat transfer in vertical cylindrical annuli filled with a porous medium, *Int. J. Heat Mass Transfer* **25**, 1755–1766 (1982).
9. V. Prasad and F. Kulacki, Natural convection in a vertical porous annulus, *Int. J. Heat Mass Transfer* **27**, 207–219 (1984).
10. V. Prasad, Numerical study of natural convection in a vertical porous annulus with constant heat flux on the inner wall, *Int. J. Heat Mass Transfer* **29**, 841–853 (1986).
11. V. D. Murty, C. L. Clay, M. P. Camden and D. B. Paul, Natural convection in porous media in a cylindrical annulus—effect of radius ratio, *Proceedings of the International Conference on Numerical Methods*, pp. 487–496, Swansea (1989).
12. K. Muralidhar and F. A. Kulacki, Non Darcy natural convection in a saturated horizontal porous annulus, *ASME J. Heat Transfer* **110**, 133–139 (1988).
13. G. Lauriat and V. Prasad, Natural convection in a vertical porous annulus. In *Convective Heat and Mass Transfer in Porous Media*, NATO ASI Series, Series E, **196**, 143–172 (1991).
14. A. Bejan and C. L. Tien, Natural convection in a horizontal space bounded by two concentric cylinders with different end temperatures, *Int. J. Heat Mass Transfer* **22**, 919–927 (1979).
15. M. Kaviany, Non-Darcian effects on natural convection in porous media confined between horizontal cylinders, *Int. J. Heat Mass Transfer* **29**, 1513–1519 (1986).
16. V. Prasad, F. A. Kulacki and A. V. Kulkarni, Free convection in a vertical porous annulus with constant heat flux on the inner wall—experimental results, *Int. J. Heat Mass Transfer* **29**, 713–723 (1986).
17. P. Cheng and C. T. Hsu, Fully developed, forced convective flow through an annular packed sphere bed with wall effects, *Int. J. Heat Mass Transfer* **29**, 1843–1853 (1986).
18. K. Vafai, Convective flow and heat transfer in variable porosity media, *J. Fluid Mech.* **147**, 233–259 (1984).
19. D. Poulikakos and K. Renken, Analysis of forced convection in a duct filled with porous media, *ASME J. Heat Transfer* **109**, 880–888 (1987).
20. M. L. Hunt and C. L. Tien, Non-Darcian convection in cylindrical packed beds, *ASME/JSME* (1987).
21. F. C. Chou, W. Y. Lien and S. H. Lin, Analysis and experiment of non-Darcian convection in horizontal square packed sphere channels—1. Forced convection, *Int. J. Heat Mass Transfer* **35**, 195–205 (1992).
22. B. X. Wang and J.-H. Du, Forced convective heat transfer in a vertical annulus filled with porous media, *Int. J. Heat Mass Transfer* **36**, 4207–4213 (1993).
23. D. Vortmeyer and J. Schuster, Evaluation of steady flow profiles in rectangular and circular packed beds by a variational method, *Chem. Engng Sci.* **38**, 1691–1699 (1983).
24. K. Vafai and R. Thiyagaraja, Analysis of flow and heat transfer at the interface region of a porous medium, *Int. J. Heat Mass Transfer* **30**, 1391–1405 (1987).
25. D. Poulikakos and M. Kazmierczak, Forced convection in a duct partially filled with a porous material, *ASME J. Heat Transfer* **109**, 653–662 (1987).
26. G. Lauriat and K. Vafai, Forced convective flow and heat transfer through a porous medium exposed to a flat plate or a channel. In *Convective Heat and Mass Transfer in Porous Media*, NATO ASI Series, Series E, **196**, 289–327 (1991).
27. K. Vafai and S. J. Kim, Forced convection in a channel filled with a porous medium: an exact solution, *ASME J. Heat Transfer* **111**, 1103–1106 (1989).
28. W. M. Kays and M. E. Crawford, *Convective Heat and Mass Transfer* (3rd Edn), p. 139. Mc-Graw Hill, New York (1993).

## APPENDIX

Expressions of constants  $E_p$ ,  $F_p$ ,  $E_f$  and  $F_f$ 

The constants  $E_p$ ,  $F_p$ ,  $E_f$  and  $F_f$  used in equations (34) and (35) are determined using the boundary conditions equations (18). Their expressions are given below:

$$F_f = \frac{r_o r_i \Lambda}{(r_i + r_o) \bar{u}} \left\{ \frac{r_o^3}{16} + C_1 \frac{r_o}{2} \ln r_o + \left( C_2 - \frac{C_1}{2} \right) \frac{r_o}{2} \right\}$$

$$F_p = \frac{r_i \Lambda}{(r_i + r_o) \bar{u}}$$

$$\times \left\{ \frac{r_o^4 - s^4}{16} + C_1 \frac{r_o^2 - s^2}{2} \ln s + \left( C_2 - \frac{C_1}{2} \right) \frac{r_o^2 - s^2}{2} + \left[ B s \sqrt{Da} I_1(s/\sqrt{Da}) - C s \sqrt{Da} K_1(s/\sqrt{Da}) - Da \frac{s^2}{2} \right] \right\}$$

$$E_p = -F_p \ln r_i + \frac{r_i}{(r_i + r_o) \bar{u}}$$

$$\times \left\{ B Da I_0(r_i/\sqrt{Da}) + C Da K_0(r_i/\sqrt{Da}) - Da \frac{r_i^2}{4} \right\}$$

$$E_f = E_p + (F_p - F_f) \ln s - \frac{r_i}{(r_i + r_o) \bar{u}}$$

$$\times \left\{ B Da I_0(s/\sqrt{Da}) + C Da K_0(s/\sqrt{Da}) - Da \frac{s^2}{4} - \Lambda \left( \frac{s^4}{64} + C_1 \frac{s^2}{4} \ln s - (C_1 - C_2) \frac{s^2}{4} \right) \right\}$$

## Calculation of Nu

The intermediate analytical calculations of the different integrals used in evaluating the Nusselt number in equation (39) are given in the following:

$$\int x I_0(x) dx = x I_1(x)$$

$$\int x I_0(x) K_0(x) dx = \frac{x^2}{2} \{ I_0(x) K_0(x) + I_1(x) K_1(x) \}$$

$$\int x K_0(x) dx = -x K_1(x)$$

$$\int x^3 K_0(x) dx = -x^3 K_1(x) - 2x^2 K_0(x) - 4x K_1(x)$$

$$\int x I_0^2(x) dx = \frac{x^2}{2} \{I_0^2(x) - I_1^2(x)\}$$

$$\int x \ln x I_0(x) dx = x \ln x I_1(x) - I_0(x)$$

$$\int x K_0^2(x) dx = \frac{x^2}{2} \{K_0^2(x) - K_1^2(x)\}$$

$$\int x \ln x K_0(x) dx = -x \ln x K_1(x) - K_0(x)$$

$$\int x^3 I_0(x) dx = x^3 I_1(x) - 2x^2 I_0(x) + 4x I_1(x)$$